Catalysis Science & Technology

Accepted Manuscript

ROYAL SOCIETY OF CHEMISTRY

www.rsc.org/catalysis

Mechanistic Insight to Selective Catalytic Reduction of NO by NH_3 over Low-valent Titanium-porphyrin: A DFT Study

Phornphimon Maitarad,[a] Jittima Meeprasert,[b] Liyi Shi,[a] Jumras Limtrakul,[c] Dengsong Zhang[a] and Supawadee Namuangruk[b]**

[a] Research Center of Nano Science and Technology, Shanghai University, Shanghai 200444, P. R. China

[b] National Nanotechnology Center, NSTDA, 111 Thailand Science Park, Pahonyothin Road, Klong Luang, Pathum Thani 12120, Thailand

[c] Vidyasirimedhi Institute of Science and Technology, Wang Chan, Rayong 21210, Thailand

*Phone: +86-21-66137152. E-mail: dszhang@shu.edu.cn (D.Z.)

*Phone: +66- 25647100 ext 6595. E-mail: supawadee@nanotec.or.th (S.N.)

ABSTRACT

In this work, the reaction mechanism of ammonia selective catalytic reduction (NH_3-SCR) of nitric oxide over a low-valance Ti-porphyrin catalyst was studied by density functional theory (DFT) calculations for both low- and high-spin states. The reaction proceeds via *(i)* NH_3 complexation with the Ti-porphyrin complex, and its subsequent oxidation to NH_2, with a large activation barrier of 32–34 kcal/mol because of the difficulty of N-H bond dissociation. *(ii)* Bonding between NO and the NH_2 ligand forms an NH_2NO intermediate by an Eley-Rideal-type mechanism. Calculated activation energies for this step are 4.34 and 10.22 kcal/mol for the low- and high-spin states, respectively. *(iii)* Formation of NHNOH by rearrangement of the NH_2NO intermediate. Spin crossings in steps *(ii)* and *(iii)* play an important role in the overall reaction by providing a mechanism with a smaller activation energy of 17.05 kcal/mol, compared with 28.02 kcal/mol for the un-catalyzed reaction. *(iv)* In the final step, decomposition of NHNOH results in formation of N_2 and H_2O molecules, with a small energy barrier of approximately 7–9 kcal/mol. For pairwise pathway comparisons, Ti-porphyrin in the triplet state offers 8.43 kcal/mol greater stability than the singlet does, and the reaction is more likely to proceed through a high-spin pathway because of its lower relative energies compared to low spin. The obtained activation energies for NH_3-SCR of NO are comparable with theoretical results for the reduction of NO over V_2O_5 and Fe-zeolite systems. Thus, Ti-porphyrin has potential as an alternative catalyst for NH_3-SCR of nitric oxide.

Keywords: NH_3-SCR; Reaction mechanism; De-NOx, Density Functional Theory.

1. Introduction

Ammonia selective catalytic reduction (NH_3-SCR) of NO, is widely used to remove NO gas from stationary plant and diesel vehicles because of its high efficiency and economy of operation. Commercial catalysts available for NH_3-SCR of NO, the V_2O_5-$WO_3(MoO_3)/TiO_2$ catalyst systems perform best over the range of 300–400 °C. However, high-temperature operation of vanadium oxide-based catalysts has some drawbacks, including toxicity of vanadia species that are created, significant conversion of SO_2 to SO_3, and generation of N_2O, a greenhouse gas.[1-5] Consequently, there is strong interest in the development of NH_3-SCR catalysts that avoid the problems associated with existing commercial catalyst systems.

Porphyrin is an interesting compound because it readily self assembles into ordered monolayers. The molecule possesses two axial coordination sites that may function as centers of catalytic activity, or sensor functionality. Furthermore, porphyrin is well suited for anchoring to a solid substrate to form metal-porphyrin assemblies that feature in several useful applications,[6-10] including photovoltaic materials, field-responsive materials, and catalytic materials. Metal-porphyrins are potential catalysts for many commercially important redox reactions.[11-17] Yamamoto *et al*. reported that a non-metal porphyrin derivative-modified TiO_2 catalyst for photo-assisted selective catalytic reduction (photo-SCR) of nitric oxide, achieved an NO conversion of 79 % with N_2 selectivity of 100 %.[18] However, it is unclear how the porphyrin moiety and TiO_2 interact to activate NH_3 in the reaction.

We recently published a theoretical study demonstrating the potential for low-valance Ti-porphyrin as catalyst for N_2O decomposition.[19] We are interested in extending our theoretical study of the Ti-porphyrin catalyst to another decomposition of the NO_x family, namely, the NH_3-SCR of NO, for which several reaction mechanisms have been proposed.[20-24] A proposed mechanism for the molecular gas-phase NH_3-SCR of NO suggests

that the NH_2NO intermediate rearranges to NHNOH before decomposition occurs.[25] This intermediate step is absent from previous theoretical reports. DFT calculations suggest that the NH_3-SCR of NO comprises four consecutive elementary steps (Scheme 1): *(1)* NH_3 oxidation; NH_3 adsorbs to a Lewis acid site on the Ti-metal center and an NH_2 species is generated, *(2)* NH_2NO formation; an NO molecule attaches to the NH_2 to form an NH_2NO intermediate, *(3)* NHNOH formation; NH_2NO rearranges to form NHNOH. This step is absent from previous reports.[26-28] *(4)* NHNOH decomposition; the NHNOH decomposes to N_2 and H_2O molecules. Therefore, in this work, we investigate the use of low-valance Ti-porphyrin as catalyst for the NH_3-SCR of NO, and elucidate the intermediates, transition states, and the energy barriers along the potential-energy surface of the Lewis-acid-based reaction. The low- and high-spin states of the catalyst are considered throughout the reaction. The reaction mechanism and calculated energy barriers obtained from this catalyst are discussed and compared with those of two other potential catalysts: V_2O_5 and Fe-zeolite.

2. Model and Method

The catalytically active center of Ti-porphyrin is represented as a 34-atom single cluster (Fig. 1). The catalyst model contains a Ti atom coordinated by shells of porphyrin nitrogen atoms. The low-valance Ti(II)-porphyrin complex has no charge. We applied the M06-L density functional, which is specifically designed for transition metal complexes. This functional has been demonstrated to provide reasonable estimates of the energetic and electronic properties of transition metal complexes, and for organometallic and inorganometallic catalysts in particular.[29] The 6-31G(d,p) basis set was used for the N, C, O, and H atoms, and the LANL2DZ effective core potential was applied to describe the Ti core electrons. We previously used this model and method to investigate N_2O decomposition over

Ti-porphyrin.[19] All calculations were carried out using the Gaussian 09 program package.[30] All atoms in the system were fully relaxed during the geometry optimizations. We confirmed that the saddle point had only one imaginary vibration frequency at the transition state. Additionally, we compared activation energy barriers corrected with Zero-point energy ($\boldsymbol{E}_{\mathbf{a\text{-}ZPE}}$) at 298 K, with the uncorrected energies.

For the reaction energy profiles, the relative energy was calculated by:

$$\Delta E = E_{complex} - (E_{catalyst} + E_{adsorbate}) \quad (1)$$

where $E_{complex}$, $E_{catalyst}$, and $E_{adsorbate}$ are the total energies of the Ti-porphyrin-gas complex, the Ti-porphyrin intermediate, and small gas molecules (e.g., NO, NH_3, and N_2), respectively. For the reaction pathways calculated for low- and high-spin states, we examined the possibilities of spin crossing or intersystem crossing.

3. Results and Discussion

Our proposed reaction mechanism for NH_3-SCR of NO over Ti-porphyrin comprises four consecutive elementary steps (Scheme 1): *(1)* NH_3 oxidation, *(2)* NH_2NO (*nitrosamine*) formation, *(3)* NHNOH formation, and *(4)* NHNOH decomposition to H_2O and N_2;

Step1: NH_3 oxidation

$$[Cat] + NH_3 \rightarrow [Cat]\cdots NH_3$$

$$[Cat]\cdots NH_3 \rightarrow H[Cat]\text{–}NH_2$$

Step 2: NH_2NO formation

$$H[Cat]\text{–}NH_2 + NO \rightarrow H[Cat]\text{–}NH_2\cdots NO$$

$$H[Cat]\text{–}NH_2\cdots NO \rightarrow H[Cat]\text{–}NH_2\text{–}NO$$

Step 3: NHNOH formation

$$H[Cat]–NH_2–NO \rightarrow H[Cat]–NHNOH$$

Step 4: NHNOH decomposition

$$H[Cat]–NHNOH \rightarrow N_2–H[Cat] –H_2O$$

$$N_2–H[Cat] –H_2O \rightarrow H[Cat] + N_2 + H_2O$$

For the Ti-Porphyrin catalyst, we found that the high-spin state structure offers 8.43 kcal/mol greater stability than that of the low-spin state. Thus, at equilibrium, the high spin state structure will be dominant. However, the difference in energy between the two states is not sufficient to disregard either of them, and thus, we studied the reaction mechanisms for both spin states. Because the details of the reaction mechanisms are similar for both states, we discuss in detail only the high spin state reaction pathway.

3.1 NH_3 Oxidation

The proposed catalytic cycle begins with oxidation of NH_3 over the low-valance Ti-porphyrin catalyst (Fig. 2). NH_3 adsorbs to the Lewis acid site of ^{3}**Ti-porphyrin** to form the ^{3}**Ti**−**NH$_3$** adduct, with a calculated adsorption energy of −51.64 kcal/mol, and an intermolecular distance of 2.20 Å. In the transition state, ^{3}**TS1**, a hydrogen atom from the adsorbed NH_3 approaches a porphyrin nitrogen atom to a distance of 1.22 Å. Transition state ^{3}**TS1** has one imaginary frequency at -1062*i* cm^{-1}, which represents the motion during N−H bond cleavage. The NH_3 oxidation process has an activation energy ($\boldsymbol{E}_{\mathbf{a1}}$) of 35.45 kcal/mol. We applied Zero-point energy at 298 K to correct the activation energy ($\boldsymbol{E}_{\mathbf{a\text{-}ZPE}}$), and found $\boldsymbol{E}_{\mathbf{a1\text{-}ZPE}}$ to be 32.43 kcal/mol, slightly less than the uncorrected value. The high barrier energy calculated for this endothermic step results from the difficulty of N-H bond dissociation. At final product of this step, the Ti-NH_2 adduct has a bond distance of 1.92 Å.

3.2 NH_2NO formation

During the NH_3-SCR of NO, the **^{3}TiH-NH_2** intermediate interacts with doublet state NO to form the key intermediate, **^{4}TiH-NH_2NO** (Fig. 3). NO adsorbs to **^{3}TiH-NH_2** with an adsorption energy of -6.04 kcal/mol. The $H_2N\cdots NO$ intermolecular distance is 2.43 Å. In this second transition state (**^{4}TS2**), the $ON\cdots NH_2$ intermolecular distance is 1.69 Å. The **^{4}TS2** energy barrier ($\boldsymbol{E}_{\mathbf{a2}}$) is just 9.20 kcal/mol ($\boldsymbol{E}_{\mathbf{a2\text{-}ZPE}}$ = 10.22 kcal/mol). Finally, a new N–N bond forms with an N-N bond distance of 1.46 Å to form the H_2N-NO intermediate (**^{4}TiH-NH_2NO)**. The formation of NH_2NO is a thermodynamically favorable process.

3.3 NHNOH formation

The **^{4}TiH-NH_2NO** structure is rather constrained because of its three-membered ring configuration (Fig. 4). Its transformation to **^{4}TiH-NHNOH** proceeds via a third transition state, **^{4}TS3** (Scheme 1). The imaginary frequency at 1636*i* cm^{-1} arises from vibrational motion associated with N-H cleavage and O-H formation. This step has an energy barrier ($\boldsymbol{E}_{\mathbf{a3}}$) of 31.49 kcal/mol, and a $\boldsymbol{E}_{\mathbf{a3\text{-}ZPE}}$ corrected value of 28.02 kcal/mol). The TS3 structure features an NNOH four-membered ring ligated to Ti. The N–O bond is elongated from 1.26 Å in TiH-NH_2NO to 1.45 Å in transition state. The Ti active center bound to the O, N, and NH moieties with average bond distances of approximately 2 Å. In the following step, dissolution of the bridging hydrogen atom from nitrogen yields **^{4}TiH-NHNOH,** with a large exothermic energy of -61.67 kcal/mol. Thus, step 3 (Scheme 1) accomplishes transformation of the NH_2NO intermediate to NHNOH, after which follows a facile rearrangement and elimination of N_2 and H_2O.

3.4 NHNOH decomposition

The final step in the NH_3-SCR of NO is decomposition of NHNOH to N_2 and H_2O (Fig. 5). After formation of the **^{4}TiH-NHNOH** intermediate, rearrangement to the **^{4}TS4** transition

state (imaginary frequency = 1060*i*cm^{-1}) has a small activation energy (E_{a4}) of 8.53 kcal/mol ($E_{a4\text{-}ZPE}$ = 8.79 kcal/mol). During this process, the NHN hydrogen atom migrates toward the OH group. The HO···HNN intermolecular distance closes to 1.32 Å, suggesting the formation of H_2O. Additionally, the N–N bond distance is shortened to 1.17 Å, that of free N_2 gas. Thus, in the final step, the H_2O and N_2 molecules are produced over the TiH active center, as suggested by the **^{2}TiH-N$_2$-H$_2$O** structure. Desorption energies for N_2 and H_2O are 0.02 and 20.17 kcal/mol, respectively, implying that the catalyst has high selectivity toward N_2.

^{4}TiH (Scheme 1, step 4) is the final intermediate in our proposed mechanism. This species may (*i*) repeat the catalytic cycle, facilitating NH_3-SCR of NO by a similar reaction mechanism to that described above, or (*ii*) the complex may regenerate the Ti-porphyrin catalyst by reaction with oxidizing agents such as O_2, ammonia, or water, which are generally present in the NH_3-SCR system.[31] We propose that catalytic regeneration of **TiH** proceeds via an ammonia-based redox process: TiH + NH_3 → Ti-porphyrin + NH_4.

(More details are available in supporting information, SI).

3.5 Full reaction pathway for NH_3-SCR of NO over singlet or triplet-spin-state Ti-porphyrin catalyst

To elucidate the most favorable reaction route, Figure 6 shows overlaid plots of energy pathways for NH_3-SCR of NO over both low- and high-spin-state Ti-porphyrin. Because of its greater stability when compared with **^{1}Ti-porphyrin**, all of the displayed energies are relative to the **^{3}Ti-porphyrin** total energy (Fig. 6). All of the optimized geometries for the low- and high-spin-state systems, including the parameters used, are available in SI. A pairwise potential-energy-surface comparison reveals that the high-spin-state reaction mechanism proceeds at lower relative energies until the NH_2NO TS2 transition state. Spin

crossing occurs twice. The first spin crossing occurs during the **NO-^{4}TiH-NH2→^{2}TS2** transition, in which the high-spin state crosses to lower energy than the low-spin state. The second occurrence of spin crossing occurs after water desorption, during the **^{2}TiH-H2O→^{4}TiH** transition; the high-spin state returns to the high-energy position after release of H_2O from the active center. Thus, spin crossing influences the transformation of the NH_2NO intermediate by significantly lowering the activation barrier for the high-spin transition state (**TS3**) from 28.02 to 17.05 kcal/mol. This clearly shows that transformation of the nitrosamine intermediates adopts a low-spin-state configuration. We conclude that the high-spin-state plays an important role in the NH_3-SCR of NO over Ti-porphyrin, and that spin crossing facilitates the formation of NHNOH.

3.6 Comparison of the Ti-porphyrin theoretical energy barrier with those of other candidate catalysts.

There are few literature reports of theoretical studies into Lewis acid reaction mechanisms for NH_3-SCR of NO available for comparison. DFT/PBE calculations describing the application of the V_2O_5/TiO_2 periodic model to the NH_3-SCR of NO revealed that the rate-determining step is the deprotonation of NH_3, with an energy barrier of approximately 30 kcal/mol.[28] An NH_2NO intermediate forms via a concerted mechanism, with the activation energy for N–N bond formation being just 5 kcal/mol, relative to the NH_2 intermediate. Furthermore, a V_2O_5 surface cluster model for the NH_3-SCR of NO mechanism has been also intensively studied by using B3LYP/6-31G(d)// B3LYP/6-311++G(2d,2p).[26] As with the Lewis site mechanism, NH_3 coordinates to the vanadium atom followed by dissociation and bonding of a hydrogen atom to an oxygen at the cluster surface. This results in formation of a V-NH_2 intermediate species with an energy barrier of 51.3 kcal/mol. In the next step, NO combines with the coordinated NH_2 species to form NH_2NO, with an energy barrier of only 0.1 kcal/mol. In an

alternative mechanism, the NH_2NO forms spontaneously in a conserved process, which agrees well with the energy obtained for the V_2O_5/TiO_2 model by periodic calculation. The Fe-zeolite catalyst has potential for NH_3-SCR application. The Fe-modified zeolite model (Z-$[FeO]^+$) reaction mechanism was investigated at the B3LYP/TZVP level of theory.[32] It is probable that NH_3 adsorbs on Z-$[FeO]^+$ followed by transfer of a proton to form Z-$[NH_2FeOH]^+$ with an activation barrier of 23.3 kcal/mol. Subsequently, the complex reacts with NO to form the NH_2NO intermediate, with an energy barrier of 3.4 kcal/mol, which is similar to the V_2O_5 catalytic calculation results.

Applying the cluster model with the MO6L functional reveals that the energy barriers for singlet- and triplet-state Ti-porphyrin catalyzed oxidation of NH_3 fall in the range 32–34 kcal/mol. This result is comparable with the energy barriers seen for V_2O_5/TiO_2 and Fe-zeolite catalysts. ^{1}Ti-porphyrin requires only 4.34 kcal/mol activation energy for the NH_2NO formation step, while ^{3}Ti-porphyrin has an activation energy of 10.22 kcal/mol. The NH_2NO formation energy over ^{1}Ti-porphyrin is similar to those of V_2O_5 and Fe-Zeolite catalysts, while its formation over ^{3}Ti-porphyrin is more endothermic. Previous calculations did not involve formation of NHNOH prior to N_2 and H_2O production. However, this is a necessary step after formation of the NH_2NO intermediate, particularly for the Ti-porphyrin catalyst because of the reduction in activation energy to 17.05 kcal/mol that occurs after spin crossing; this reduces the energy barrier for decomposition to N_2 and H_2O to 7-9 kcal/mol. Consequently, we propose, Ti-porphyrin as an alternative to commercial catalysts V_2O_5 and Fe-zeolite for NH_3-SCR of NO, based on our comparison of theoretical activation energy calculations.

Conclusion

We used DFT calculations to explore the mechanism of NH_3-SCR of NO over low- and high-spin state Ti-porphyrin using DFT calculations. The proposed reaction mechanism is an energetically favorable process, comprising four consecutive elementary steps. The activation barrier (*i*) for NH_3 oxidation is 32.43 kcal/mol ($\boldsymbol{E_{a1\text{-}ZPE}}$), (*ii*) for formation of NH_2NO is 10.22 kcal/mol ($\boldsymbol{E_{a2\text{-}ZPE}}$), (*iii*) for NHNOH formation is 17.05 kcal/mol ($\boldsymbol{E_{a3\text{-}ZPE}}$), and (*iv*) for decomposition of NHNOH is 8.79 kcal/mol ($\boldsymbol{E_{a4\text{-}ZPE}}$). The N─H bond cleavage that occurs during oxidation of NH_3 is the rate-limiting step for both singlet and triplet spin states, because it has the greatest activation barrier (32-34 kcal/mol), which is in good agreement with previous reports.[26,28,32] Adsorption of NO on the coordinated NH_2 to form the NHNOH intermediate is thermodynamically favorable, and the subsequent decomposition of NHNOH to N_2 and H_2O is a facile process. Release of N_2 from the catalyst has a very small desorption energy (less than 1 kcal/mol), suggesting that this catalyst provides good N_2 selectivity. The obtained activation energy barriers for the NH_3-SCR process are comparable to those of the commercially available V_2O_5 and Fe-zeolite catalysts, and thus low-valance Ti-porphyrin is a potential catalyst for NH_3-SCR of NO.

ACKNOWLEDGEMENTS

The authors acknowledge the support of the National Basic Research Program of China (973 Program, 2014CB660803), the National Natural Science Foundation of China (U1462110), and the Shanghai Municipal Education Commission (14ZZ097). The authors would like to thank the National Research Council of Thailand (NRCT) and the National Nanotechnology Center for financial support through the "Flagship Clean Air Program". Finally, we thank the Nanoscale Simulation Laboratory at the National Nanotechnology Center (NANOTEC), Thailand for computing resources.

Supporting Information

† Electronic supplementary information (ESI) available. See DOI: 10.1039/xxxxxxx

Notes

The authors declare no competing financial interests.

REFERENCES

(1) R. Q. Long and R. T. Yang, *J. Am. Chem. Soc*., 1999, 121, 5595-5596.

(2) S. Roy and A. Baiker, *Chem. Rev*., 2009, 109, 4054-4091.

(3) G. Busca, L. Lietti, G. Ramis and F. Berti, *Appl. Catal. B: Environ*., 1998, 18, 1-36.

(4) Y. Zheng, A. D. Jensen and J. E. Johnsson, *Appl. Catal. B: Environ*., 2005, 60, 253-264.

(5) M. Fu, C. Li, P. Lu, L. Qu, M. Zhang, Y. Zhou, M. Yu and Y. Fang, *Catal. Sci. Technol*., 2014, 4, 14-25.

(6) N. U. Day, M. G. Walter and C. C. Wamser, *J. Phys. Chem. C*, 2015, 119, 17378–17388.

(7) E. D. Sternberg, D. Dolphin and C. Brückner, *Tetrahedron*, 1998, 54, 4151–4202.

(8) J. H. Fuhrhop, *Langmuir*, 2014, 30, 1–12.

(9) J. S. Lindsey, *New J. Chem*., 1991, 15, 153-180.

(10) K. S. Suslick, N. A. Rakow, M. E. Kosal and J. H. Chou, *J. Porphyrins Phthalocyanines,* 2000, 4, 407-413.

(11) W. M. Campbell, K. W. Jolley, P. Wagner, K. Wagner, P. J. Walsh, K. C. Gordon, L. Schmidt-Mende, M. K. Nazeeruddin, Q. Wang, M. Grätzel and D. L. Officer, *J. Phys. Chem. C. Lett.* 2007, 111, 11760-11762.

(12) J. Harvey, *Coordin. Chem. Rev.,* 2003, 247, 1-19.

(13) F. Scandola, C. Chiorboli, A. Prodi, E. Iengo and E. Alessio, *Coordin. Chem. Rev.,* 2006, 250, 1471-1496.

(14) N. Cheng, C. Kemna, S. Goubert-Renaudin and A. Wieckowski, *Electrocatal.,* 2012, 3, 238-251.

(15) T. Karpuschkin, M. M. Kappes and O. Hampe, *Angew. Chem. Int. Ed.,* 2013, 52, 10374-10377.

(16) H. Brand and J. Arnold, *Coordin. Chem. Rev.,* 1995, 140, 137–168.

(17) J. Rochford, D. Chu, A. Hagfeldt and E. Galoppini, *J. Am. Chem. Soc.*, 2007, 129, 4655–4665.

(18) A. Yamamoto, Y. Mizuno, K. Teramura, S. Hosokawa, T. Shishido and T. Tanaka, *Catal. Sci. Technol.*, 2015, 5, 556-561.

(19) P. Maitarad, S. Namuangruk, D. Zhang, L. Shi, H. Li, L. Huang, B. Boekfa and M. Ehara, *Environ. Sci. Technol.*, 2014, 48, 7101–7110.

(20) W. S. Kijlstra, D. S. Brands, E. K. Poels and A. Bliek, *J. Catal.*, 1997, 171**,** 208–218.

(21) W. S. Kijlstra, D. S. Brands, H. I. Smit, E. K. Poels and A. Bliek, *J. Catal.*, 1997, 171, 219–230.

(22) G. Marbán, T. Valdés-Solís and A. B. Fuertes, *J. Catal*., 2004, 226, 138–155.

(23) G. Qi and R. T. Yang, *J. Phys. Chem. B,* 2004, 108*,* 15738-15747.

(24) G. Qi, R. T. Yang and R. Chang, *Appl. Catal. B: Environ.*, 2004, 51, 93–106

(25) D. Sun, W. F. Schneider, J. B. Adams and D. Sengupta, *J. Phys. Chem. A,* 2004**,** 108*,* 9365-9374.

(26) R. Yuan, G. Fu, X. Xu and H. Wan, *Phys. Chem. Chem. Phys.,* 2011, 13, 453–460.

(27) S. Heinbuch, F. Dong, J. J. Rocca and E. R. Bernstein, *J. Chem. Phys.,* 2010, 133, 174314-1-11.

(28) A. Vittadini, M. Casarin and A. Selloni, *J. Phys. Chem. B,* 2005, 109*,* 1652-1655.

(29) Y. Zhao and D. G. Truhlar, *Theor. Chem. Account*, 2008, 120, 215–241.

(30) M. J. Frisch, G. W. Trucks, H. B. Schlegel, G. E. Scuseria, M. A. Robb, J. R. Cheeseman, G. Scalmani, V. Barone, B. Mennucci, G. A. Petersson, H. Nakatsuji, M. Caricato, X. Li, H. P. Hratchian, A. F. Izmaylov, J. Bloino, G. Zheng, J. L. Sonnenberg, M. Hada, M. Ehara, K. Toyota, R. Fukuda, J. Hasegawa, M. Ishida, T. Nakajima, Y. Honda, O. Kitao, H. Nakai, T. Vreven, J. A. Montgomery, Jr., J. E. Peralta, F. Ogliaro, M. Bearpark, J. J. Heyd, E. Brothers, K. N. Kudin, V. N. Staroverov, R. Kobayashi, J. Normand, K. Raghavachari, A. Rendell, J. C. Burant, S. S. Iyengar, J. Tomasi, M. Cossi, N. Rega, J. M. Millam, M. Klene, J. E. Knox, J. B. Cross, V. Bakken, C. Adamo, J. Jaramillo, R. Gomperts, R. E. Stratmann, O. Yazyev, A. J. Austin, R. Cammi, C. Pomelli, J. W. Ochterski, R. L. Martin, K. Morokuma, V. G. Zakrzewski, G. A. Voth, P. Salvador, J. J. Dannenberg, S.

Dapprich, A. D. Daniels, Ö. Farkas, J. B. Foresman, J. V. Ortiz, J. Cioslowski, and D. J. Fox, *Gaussian, Inc., Wallingford CT*, 2009.

(31) W. Song, J. Liu, H. Zheng, S. Ma, Y. Wei, A. Duan, G. Jiang, Z. Zhao and E. J. M. Hensen, *Catal. Sci. Technol*., 2016, DOI: 10.1039/c5cy01597a.

(32) T. C. Brüggemann and F. J. Keil, *J. Phys. Chem. C,* 2011, 115, 23854–23870.

322 **Table 1.** Comparison of the activation energies for NH_3-SCR of NO assuming the Lewis acid
323 reaction mechanism, over commercial V_2O_5, potential Fe-zeolite, and Ti-porphyrin catalysts.

	Energy (kcal/mol)			
	NH_3 oxidation	NH_2NO formation	NHNOH formation	N_2 and H_2O production
V_2O_5/TiO_2 periodic model[a]	30	5		
V_2O_5 cluster model[b]	51.3	0.1		
Fe-zeolite[c]	23.3	3.4		
^{1}Ti-porphyrin	33.68	4.34	17.05	7.02
^{3}Ti-porphyrin	32.43	10.22	28.02	8.79

324 [a]Vittadini, *et al*. (ref. 28),[b] Yuan *et al*. (ref. 26), [c] Brüggemann *et al*. (ref 32)
325
326
327
328
329
330
331
332
333
334
335
336
337
338
339

Figure Captions

Scheme 1: Proposed reaction mechanism for Selective Catalytic Reduction of NO by NH_3 over Ti-porphyrin. Steps consist of NH_3 oxidation (Step 1), NO insertion and NH_2NO formation (Step 2), NHNOH formation (Step 3), and NHNOH decomposition to H_2O and N_2 (Step 4).

Figure 1. Model of Ti-porphyrin catalyst (a) top view and (b).side view.

Figure 2. NH_3 oxidation over high-spin-state Ti-porphyrin.

Figure 3. NH_2NO intermediate formation over high-spin-state Ti-porphyrin.

Figure 4. NHNOH intermediate formation over high-spin state Ti-porphyrin.

Figure 5. NHNOH decomposition to nitrogen and water molecules over high-spin-state Ti-porphyrin.

Figure 6. Energy profile comparison for low-spin and high-spin reaction routes in the NH_3-SCR of NO over a Ti-porphyrin catalyst.

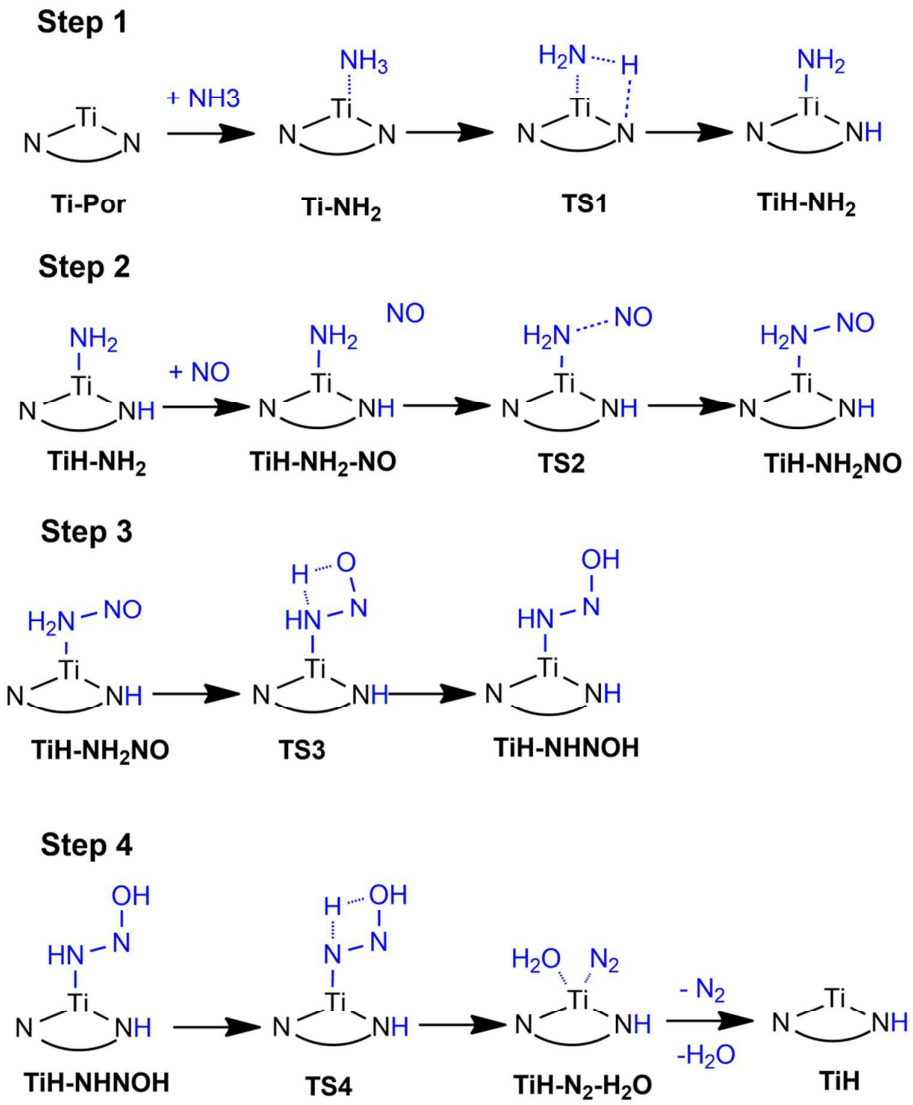

355

356 **Scheme 1:** Proposed reaction mechanism for the selective catalytic reduction of NO by NH_3
357 over a Ti-porphyrin catalyst comprising: (Step 1) NH_3 oxidation, (Step 2) NO insertion and
358 NH_2NO formation, (Step 3) NHNOH formation, and (Step 4) NHNOH decomposition to H_2O
359 and N_2.

360

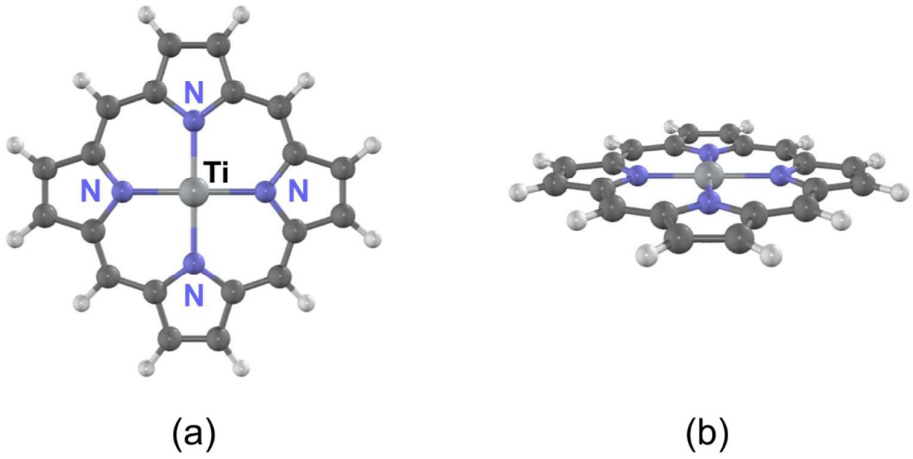

361

362 **Figure 1.** Model of low valance Ti-porphyrin catalyst in (a) top view and (b) side view.

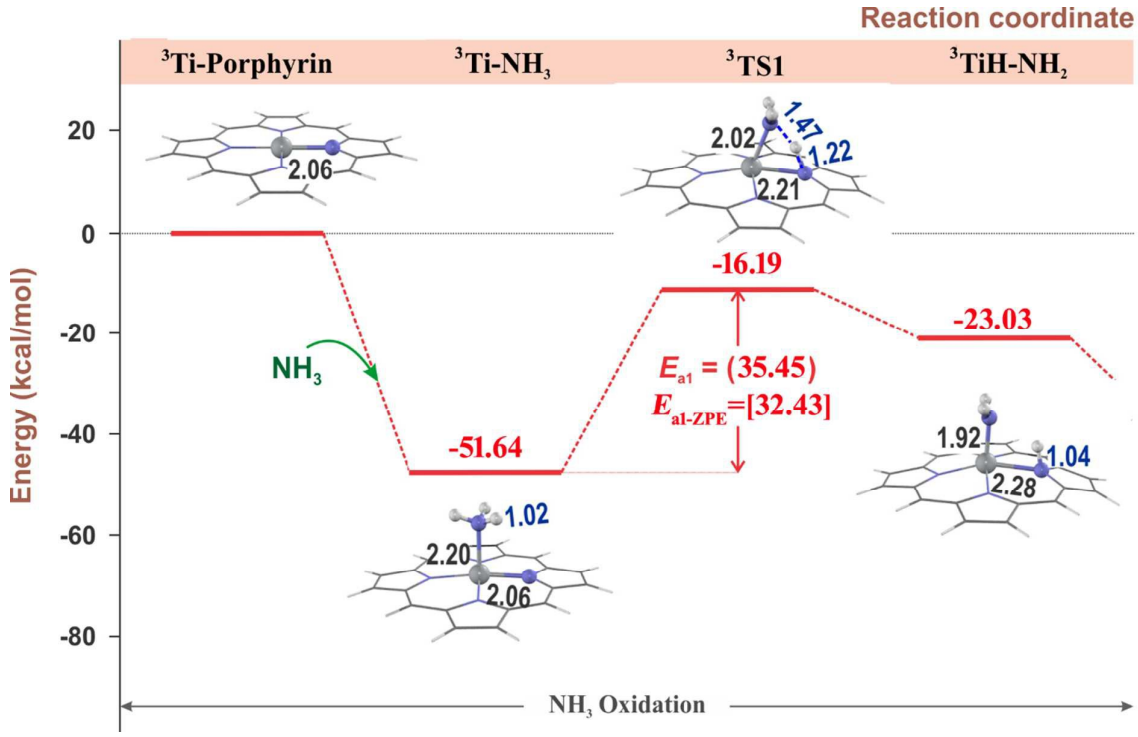

363

364 **Figure 2**. NH_3 oxidation over high-spin-state Ti-porphyrin.

365

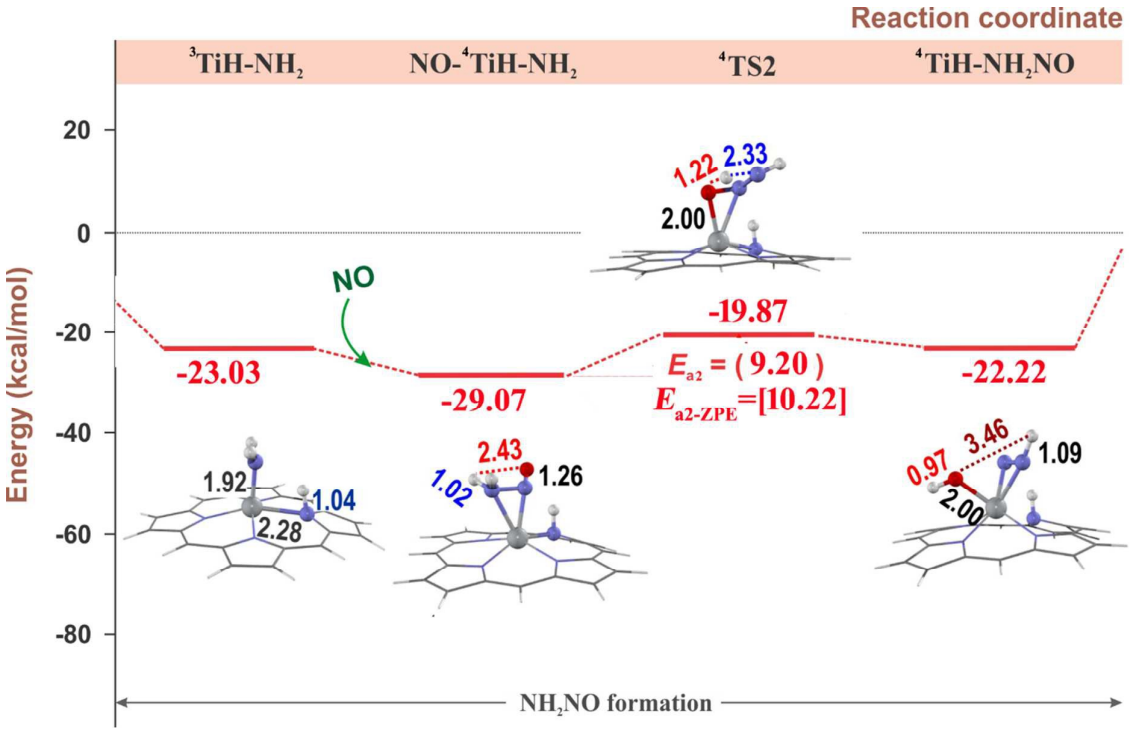

366

367 **Figure 3**. formation of NH_2NO intermediate over high-spin-state Ti-porphyrin.

368

369

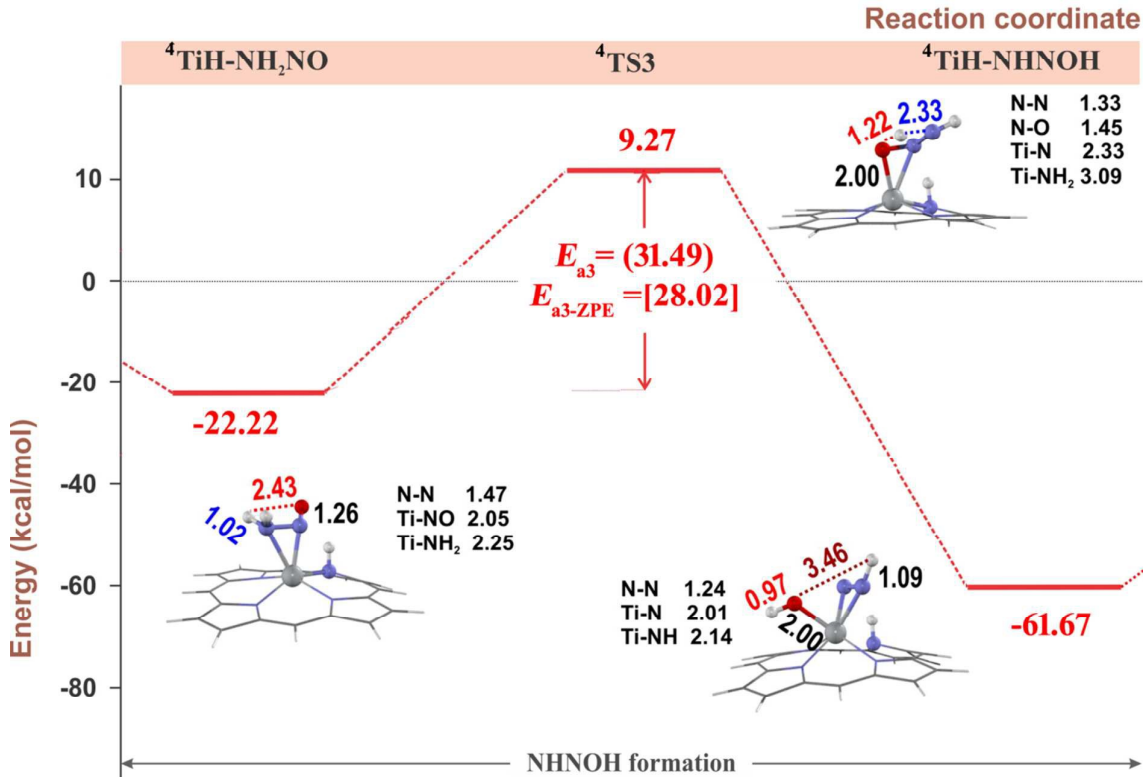

Figure 4. NHNOH intermediate formation over high-spin-state Ti-porphyrin.

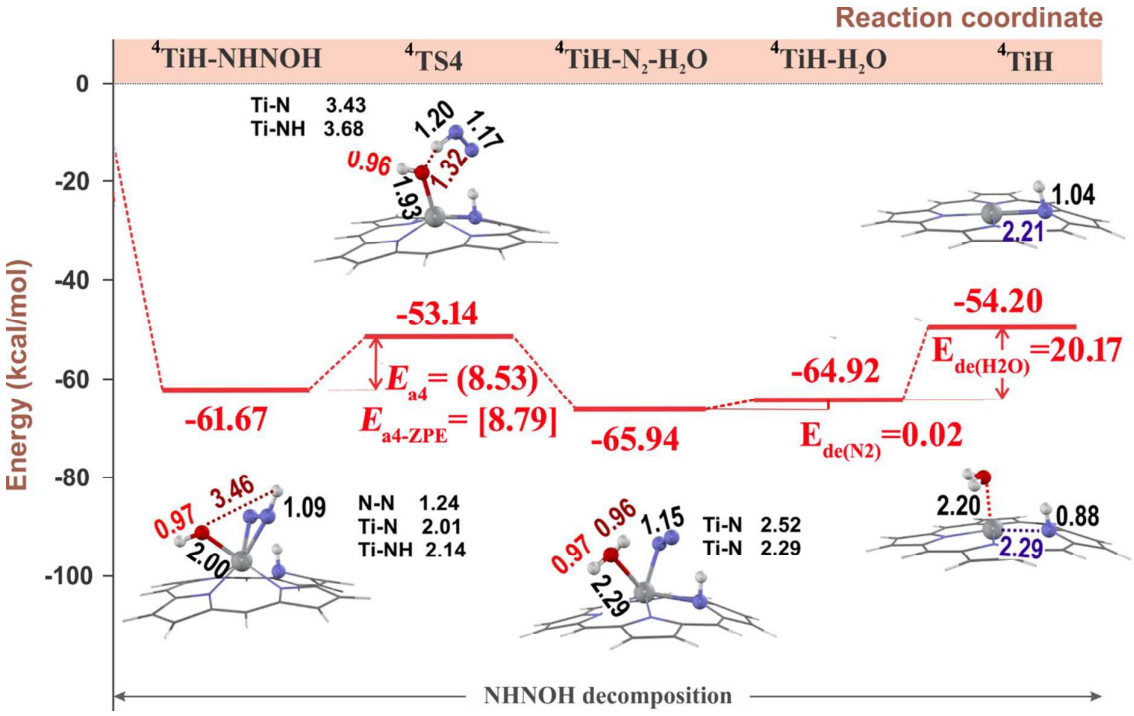

373

374 **Figure 5.** NHNOH decomposition to nitrogen and water over high-spin-state Ti-porphyrin.

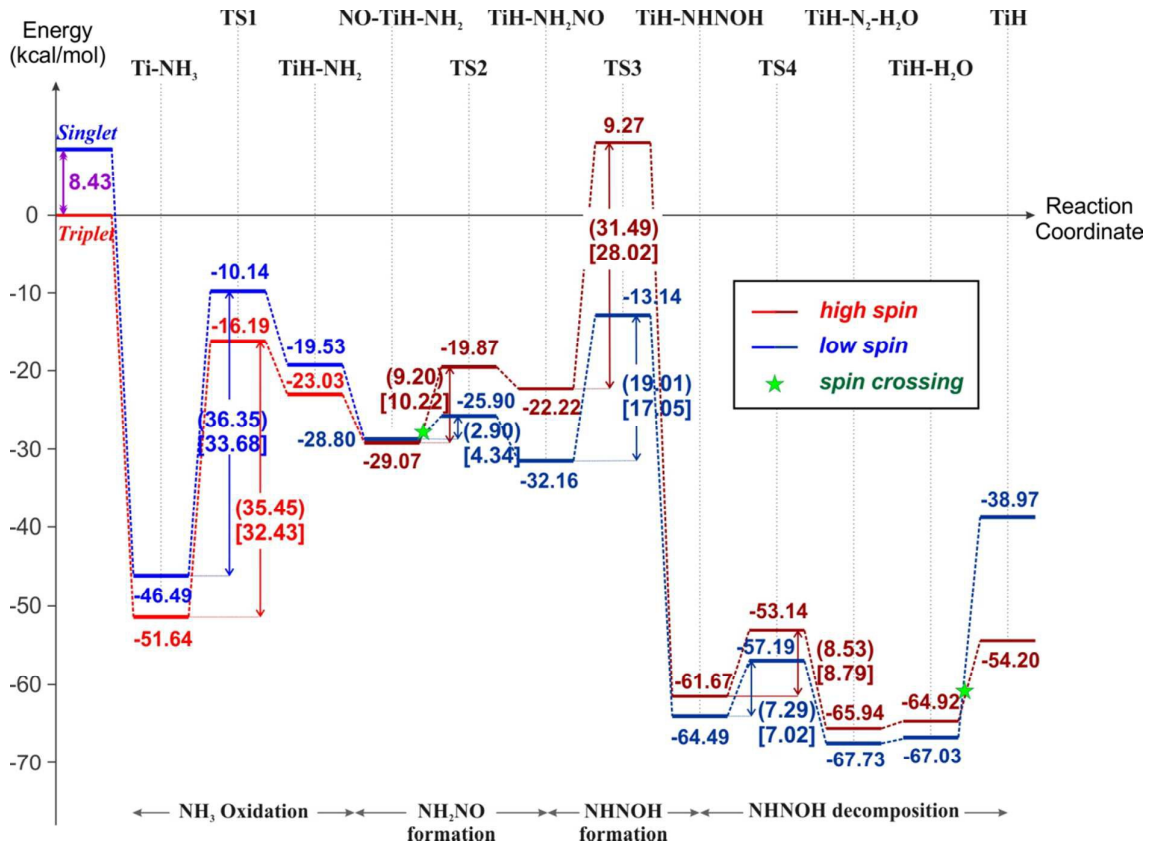

Figure 6. Comparison of energy profiles for low-spin and high-spin reaction routes in the NH_3-SCR of NO over a Ti-porphyrin catalyst.

382 **Table of content**

383

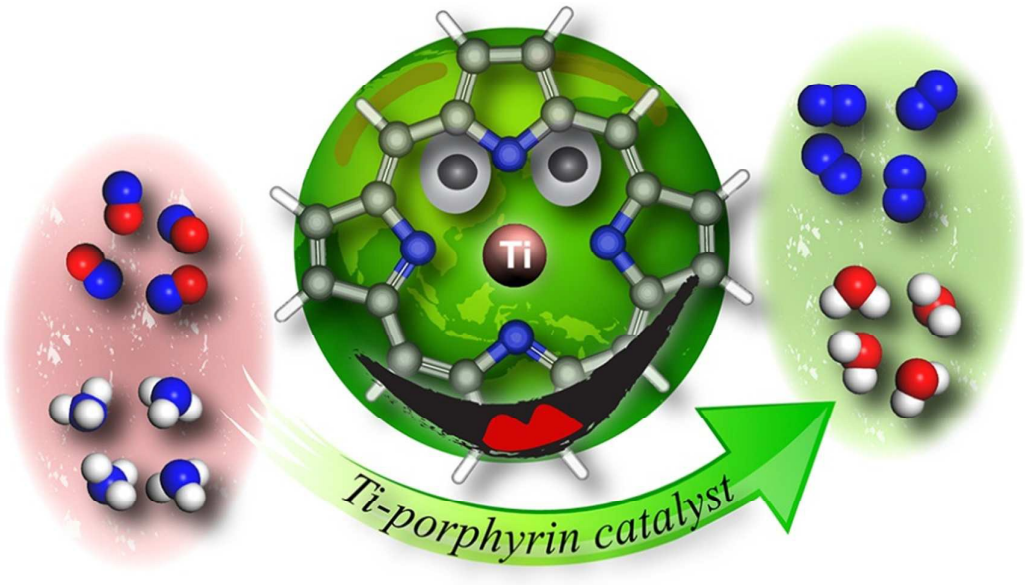

384

385 The theoretical study shows Ti-porphyrin has potential as an alternative catalyst for NH_3-

386 SCR of NO.

387

388

389

390